Electrochimica Acta 378 (2021) 138143

Contents lists available at ScienceDirect

Electrochimica Acta

journal homepage: www.elsevier.com/locate/electacta

First principle modeling of a silicene anode for lithium ion batteries

A.Y. Galashev[a,b,*], A.S. Vorob'ev[a]

[a] Institute of High-Temperature Electrochemistry, Ural Branch, Russian Academy of Sciences, Sofia Kovalevskaya Str. 22, Yekaterinburg 620990, Russia
[b] Ural Federal University named after the first President of Russia B.N. Yeltsin, Mira Str., 19, Yekaterinburg 620002, Russia

ARTICLE INFO

Article history:
Received 30 October 2020
Revised 30 December 2020
Accepted 9 March 2021
Available online 12 March 2021

Keywords:
Band structure
Gravimetric capacities
Lithium
Silicene
Voltage profile

ABSTRACT

This work is devoted to a first principle study of changes in the structural, energy, and electronic properties of a silicene anode, represented by a bilayer silicene, as it is filled with lithium. The parallel folded silicene sheets form a flat channel with an initial gap of 0.75 nm. Lithium atoms were deposited both inside and outside the channel. The ratio of the amount of lithium to silicon varied in the range from 0.1 to 2.3. The maximum number of lithium atoms in the channel is revealed, which does not lead to defect formation in the silicene walls. The types of clusters in the formed packing of lithium atoms are defined and their stability is investigated. The tensile limit of silicon bonds in silicene sheets is found. The cohesive energy between the surfaces formed by lithium and the walls of the silicene channel has been established at various ratios of lithium to silicon. The change in the volume of the silicene channel is calculated depending on the amount of lithium deposited on it. The gravimetric capacities for different degrees of filling of the silicene anode with lithium were obtained. The voltage profile of the simulated anode was determined. The conductor-semiconductor and semiconductor-conductor transitions were found when the silicene channel was filled with lithium.

1. Introduction

Features of the electronic structure allow us to consider silicene as an important material for use in microelectronic devices [1]. With respect to other two-dimensional materials, silicene has a more direct way to be introduced into semiconductor technology based on the use of crystalline silicon. Silicene has beneficial biocompatibility effects and can be used for diagnostic imaging and photo-triggered therapeutics [2]. Strong adhesion of silicene to the metal, its chemical stability and high charge capacity and mobility of charge carriers determine silicene as one of the best materials for the anode of lithium-ion batteries (LIB) [3–5].

Rechargeable lithium-ion batteries power a wide variety of devices. They are used in both portable electronic devices and electric vehicles. It is possible to increase the specific capacitance LIB by using new materials for negative electrodes (anodes). Silicon is one of the best anode materials. It has a very high theoretical capacity (up to 4200mAh g^{-1}). However, during electrochemical lithiation, silicon and lithium form an alloy Li_xSi. Alloy formation leads to irreversible structural changes and is accompanied by a huge change in volume [6, 7]. In this case, significant mechanical stresses arise, which ultimately destroy the anode [8]. Already during the first reaction cycle, a solid electrolyte interface layer (SEI) is formed [9, 10]. The life cycle of the silicon anode can be increased by replacing bulk silicon with thin silicon films. Films with thicknesses in the nanometer range are especially attractive [11]. The use of thin films significantly improves the characteristics of the electrodes, increasing their resistance to cycling and significantly reducing the volumetric expansion during lithiation.

The thinnest silicon films of monoatomic thickness were obtained on both metallic and nonmetallic substrates. In silicene, as in graphene, hexagonal rings are present. However, the arrangement of Si atoms in silicene is not flat. Some atoms leave the plane at a distance from 0.06 to 0.08 nm [12]. There is a high probability of chemical interaction between Si atoms and substrate atoms. Probably as a result of this, silicene has not yet been separated from the substrate.

It was shown in a number of works that there is a significant margin of safety for a two-dimensional silicon material when filling the space between silicene sheets with lithium [13–15]. When vacancy defects are created in the walls of the silicene channel, its resistance to filling with lithium is still high. However, in earlier molecular dynamics studies [16–19] on filling the Si channel with lithium, the ratio of Li / Si atoms remained rather low (<0.25). When lithium is intercalated into bulk silicon, the Li / Si atom ratio reaches a limit of 4.4 [14]. However, with such a high filling with lithium, bulk silicon cannot withstand charging / discharging

* Corresponding author at: Institute of High-Temperature Electrochemistry, Ural Branch, Russian Academy of Sciences, Sofia Kovalevskaya Str. 22, Yekaterinburg 620990, Russia.
E-mail address: galashev@ihte.uran.ru (A.Y. Galashev).

https://doi.org/10.1016/j.electacta.2021.138143
0013-4686/

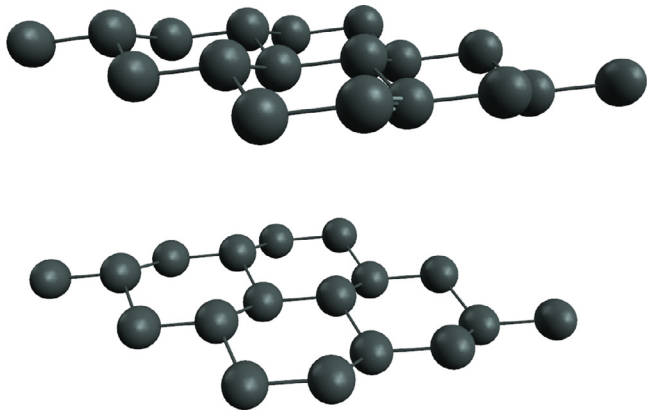

Fig. 1. Initial configuration of the silicene channel.

processes. In other words, cyclability rapidly destroys the silicon anode. The transition to thin films should correct this situation to some extent. However, a large amount of lithium in contact with the silicene film can have a destructive effect on it. As a result, the Li / Si ratio of 4.4 observed in bulk silicene can significantly decrease. Lithium accumulated in large quantities on the film surface begins to group into clusters. In this case, the collective action of Li atoms on individual Si atoms can tear them out of the film, i.e. lead to its destruction. Taking this effect into account, the limiting Li / Si ratios were established in the cases of lithization of single-layer and two-layer silicene [9, 10]. In the first case, the limiting ratio Li / Si is 1.25 [20], and in the second - 1.45 [15]. These limit values for Li / Si should be considered very approximate, since in their determination, the ratio Li / Si = 4.4 was used, which is applicable only to bulk silicon. At the same time, the establishment of a more accurate value of the limiting Li / Si ratio of silicene channel is extremely important for the design of silicene anodes.

The purpose of this work is to establish as accurate as possible the limiting value of the Li /Si ratio for silicene anodes, in the design of which flat plates made of perfect silicene are used. In addition, the task is to determine the changes in the structural, energetic and electronic properties of the silicene channel depending on the filling of the channel with lithium. All calculations were performed on a URAN cluster-type hybrid computer at the IMM UB RAS with a peak performance of 216 Tflop/s and 1864 CPU.

2. Model

The present calculations, which are based on the density functional theory (DFT), were performed without using any empirical parameters. As initial data, only information on the chemical nature of the system components was used. This approach makes it possible to accurately predict some material properties. For the calculations, the Siesta software package was used [21]. We consider a channel formed by two silicene sheets separated by a gap of 0.75 nm. The channel with such a gap was optimal for modeling lithium intercalation [13–15]. The channel used in this work is shown in Fig. 1. Each silicene sheet was represented in the form of a 3 × 3 supercell (18 silicon atoms), with two sublattices (lower and upper) separated from each other by a distance of 0.44 Å. It is this height of the buckles that was set in the DFT calculation for free-standing silicene [22]. The spatial translation period in the z-direction was 35 Å.

The study of the deposition of lithium atoms in the silicene channel was carried out as follows. Taking into account the data of [17], where the limiting Li / Si ratio was 1.45, we chose the study range for the ratio of the number of deposit lithium atoms to the number of silicon atoms from 0.1 to 2.3. Li atoms in the system

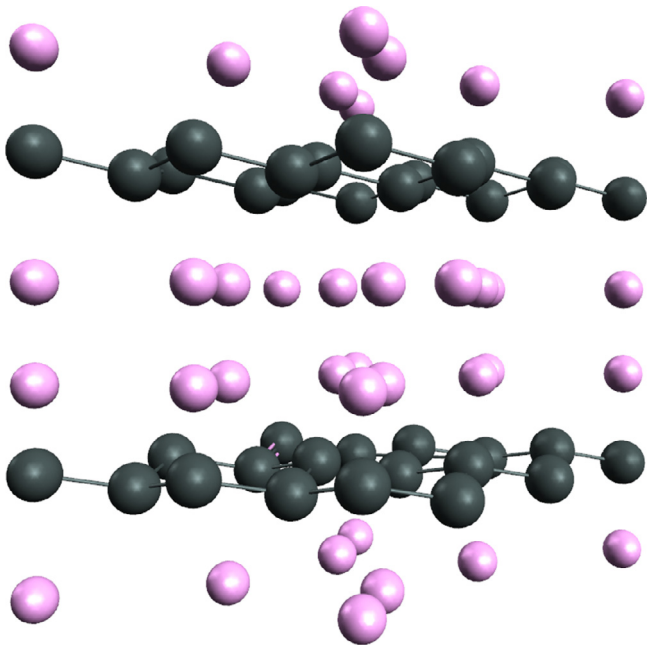

Fig. 2. The initial arrangement of lithium atoms in the silicene channel at the ratio Li / Si = 1.

could occupy the following locations: 1. the first 8 atoms were deposited in the inner volume of the channel in a position above the hexagonal rings; 2. the next eight atoms were deposited over the centers of the hexagonal rings outside the silicene channel; 3. Subsequently, the deposition took place over silicon atoms both inside and outside the channel. Fig. 2 shows an example of the arrangement of Li atoms with a Li / Si ratio of 1.

Geometric optimization using the generalized gradient approximation in the form of PBE [23] was carried out for all considered systems. The dynamic relaxation of atoms continued until the change in the total energy of the system became less than 0.001 eV. The cutoff energy of the plane wave basis set was 400 Ry. The Brillouin zone was specified by the Monkhorst-Pack method [24] using 10 × 10 × 1 k-points. After geometric optimization, the resulting systems were tested for temperature stability using first principle (*ab initio*) molecular dynamics simulations. In these calculations, the Nose-Hoover thermostat [25] was used, with the help of which the temperature was maintained at 293K. The time step length was 1 fs, and the duration of each calculation was 2000 time steps. The systems obtained after a first principle calculation were again subjected to geometric optimization. After all these procedures, the band structures in direction Γ-M-K-Γ of the systems were calculated, where points Γ, M and K are points of high symmetry in reciprocal space. Brillouin zone of unstrained silicene with high symmetry points and two paths Γ-M-K-Γ are shown in Fig. 3.

For all systems considered here, the following characteristics were calculated:

1. The specific energy of cohesion between the surfaces created by lithium and the silicene walls of the channel was determined according to the expression:

$$E_{\mathrm{Coh}}(\mathrm{Si}-\mathrm{Li}) = (E_{\mathrm{Tot}} - E_{\mathrm{Li}} - E_{\mathrm{Si}})/N, \quad (1)$$

where E_{tot} is the total energy of the entire system, E_{Li}, E_{Si} are the energies of lithium in the channel and silicene, respectively, and N is the number of atoms in the system.

2. The specific energy of cohesion between silicene sheets without taking into account the influence of lithium was determined

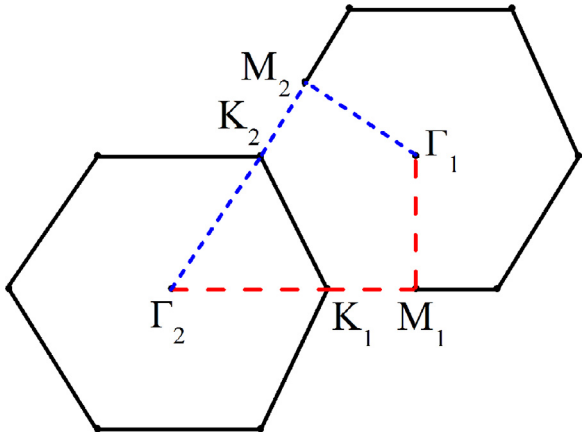

Fig. 3. Brillouin zone of unstrained silicene with high symmetry points marked; the figure shows two paths Γ-M-K-Γ.

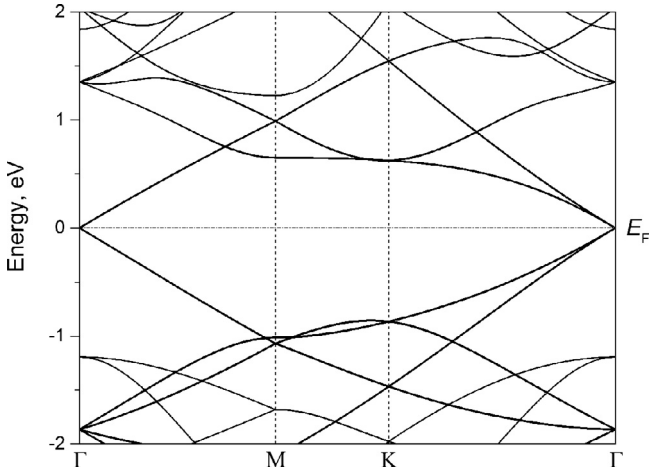

Fig. 4. Band structure for an empty silicene channel.

as:

$$E_{Coh}(Si-Si) = (E_{Tot} - E_{Sit} - E_{Sib})/N_{Si}, \quad (2)$$

where E_{Sib} and E_{Sit} are the energies calculated for the lower and upper silicene sheets, and N_{Si} is the number of silicon atoms in the system.

3. The expression for the binding energy between lithium atoms without taking into account the influence of silicene has the form:

$$E_b(Li) = (E_{Li} - N_{Li}E_{1Li})/N_{Li}, \quad (3)$$

where E_{Li} is the total energy of the lithium subsystem excluding influence of the silicene channel, E_{1Li} is the energy of a single lithium atom, and N_{Li} is the number of lithium atoms in the channel.

4. The expression for the bond energy between silicon atoms in the silicene sheet without taking into account the influence of lithium and the second silicene sheet has the form:

$$E_b(Si-Si) = (E_{Sib/Sit} - N_{Si/2}E_{1Si})/N_{Si/2}, \quad (4)$$

where $E_{Sib/Sit}$ is the total energy, calculated for the lower or upper silicene sheet, E_{1Si} is the energy, calculated for one silicon atom, and N_{Si} / 2 is the number of silicon atoms in the silicene sheet.

5. The gravimetric capacity was calculated as:

$$C_{TS} = xF/M, \quad (5)$$

where x is the number of interacting electrons, F is the Faraday number, M is the molar mass of the system.

6. The open circuit voltage was determined according to:

$$OCV = (E_{Si} + N_{Li}E_{1Li} - E_{Tot})/n_e, \quad (6)$$

where n_e is the number of valence electrons in the system.

7. The voltage for constructing a voltage profile was calculated according to the method proposed in [20,26] as:

$$V(N) = \left(E_{LiN_2Si} - E_{LiN_2Si} - (N_2 - N_1)E_{mLi}\right)/(N_2 - N_1)n_e, \quad (7)$$

where E_{LiN_2Si} and $E_{LiN_1Si}$are the total energies of systems containing N_1 and N_2 lithium atoms, and E_{mLi} is the total energy calculated for metallic lithium.

3. Results

Fig. 4 shows the band structure of a silicene channel with a gap between the walls of 7.5 Å. It can be seen from the figure that silicene in this configuration retains Dirac cones and its semiconducting properties. The bond lengths in silicene sheets are 2.28 Å; they coincide with those for an ideal free-standing silicene [27]. The cohesive energy between two silicene sheets is defined as 0.0002 eV. Such a low E_{Coh}(Si-Si) value indicates an extremely weak interaction of silicene sheets in this system.

The dependence of the calculated characteristics of the systems on the amount of lithium in the silicene channel is shown in tables S1–S3. Table S1 contains: 1. the average bond lengths between silicon atoms (Si-Si) in the lower (Bottom) and upper (Top) sheets of silicene; 2. the average bond lengths between silicon and lithium (Si-Li) atoms in the lower (Bottom) and upper (Top) sheets of silicene; 3. the distance between the upper and lower silicene sublattices Δz in the lower (Bottom) and upper (Top) silicene sheets; 4. average bond length between lithium atoms (Li-Li); 4. average distances between silicene sheets ΔZ. Table S2 presents the following energy characteristics of the system: 1. cohesion energy between lithium and the walls of the silicene channel (E_{coh}(Si-Li)); 2. binding energy in lithium packings (E_b(Li)); the binding energy of silicon atoms in the lower ($E_b(Si_b)$) and upper ($E_b(Si_t)$) sheets of silicene; cohesion energy between two sheets of silicene ($E_{coh}(Si_b\text{-}Si_t)$). Table S3 contains the following system characteristics: open circuit voltage (OCV); average Voronoi charge for silicon atoms (Q_v(Si)); average Voronoi charge for lithium atoms (Q_v(Li)); the total Voronoi charge calculated for lithium atoms (Q_v); band gap.

Fig. 5 shows the final geometric configurations of the silicene channels containing 4, 8, 12, and 16 lithium atoms. The adsorption of 4 to 16 lithium atoms in the channel brings the silicene sheets closer to 2.36-2.59 Å. In this case, the average bond length between the silicon atoms of the lower and Si atoms of the upper sheet is ~ 2.571 Å. The obtained ΔZ value is close to the bond lengths 2.41 and 2.75 Å obtained in [28] for two-layer silicene of various configurations. With the absorption of four lithium atoms, the cohesion energy between silicene sheets is -0.306 eV. An increase in the number of lithium atoms in the silicene channel leads to an increase in the distance and specific energy of cohesion between the silicene sheets. Thus, upon the adsorption of 20 lithium atoms in the channel, the cohesion energy between two silicon sheets increases to -0.032 eV and remains high upon the subsequent addition of Li atoms. This indicates a very weak interaction between the walls of the silicene channel when more than 20 lithium atoms are adsorbed.

Fig. 6 shows the dependence of the average bond lengths of Si-Si and the specific bond energies of silicon for the lower and upper sheets of silicene depending on the ratio of lithium to silicon in the system. Open squares and circles in the figure represent the data obtained for systems containing a defective silicene sheet. It is seen

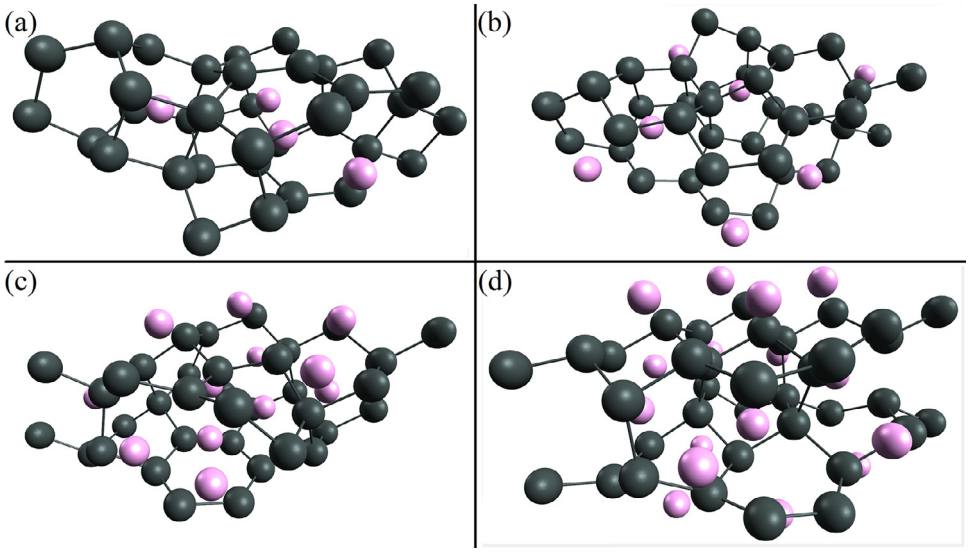

Fig. 5. Geometrical structures of the systems "silicene channel with lithium" during absorption: (a) 4, (b) 8, (c) 12 and (d) 16 lithium atoms.

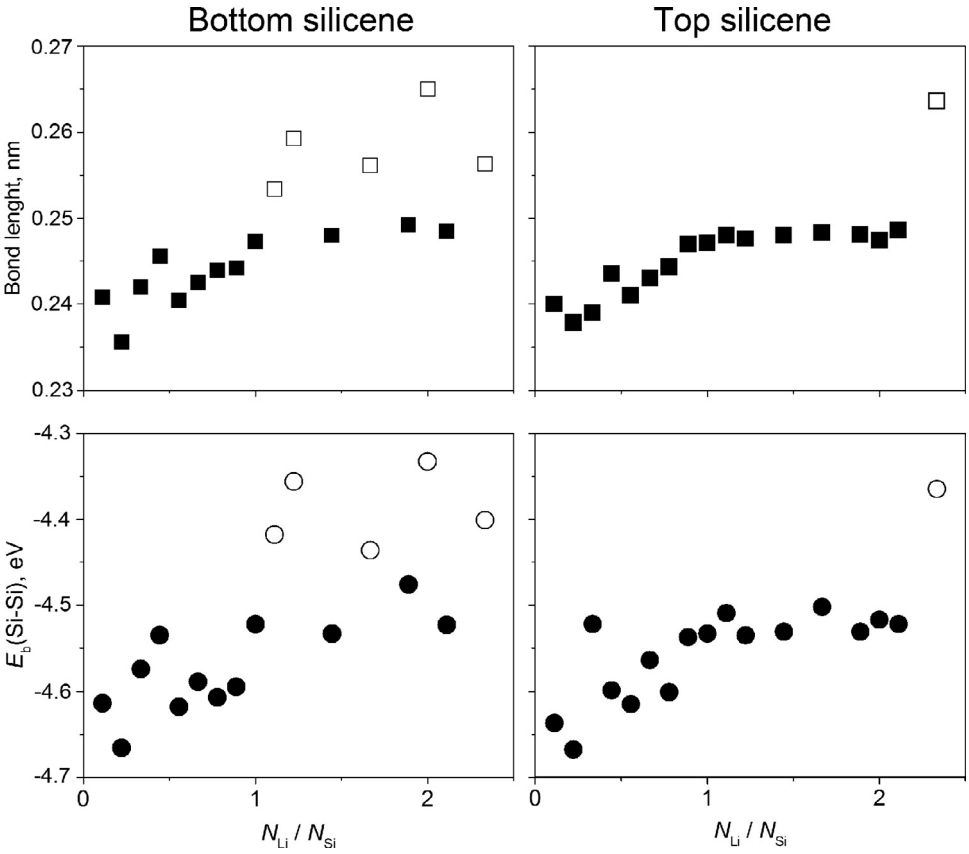

Fig. 6. Average lengths and specific bond energies in the upper and lower silicene sheets depending on the ratio of lithium atoms to the silicon atoms, open squares and circles denote the characteristics obtained for defective silicene sheets.

that the formation of a defect in silicene leads to an increase in the average length and specific binding energy in the silicene sheet. There is a direct relationship between the specific binding energy and the bond length in silicene sheets. The specific binding energy for the top and bottom sheets of silicene without lithium absorption in the channel is -4.789 eV. The absorption of lithium atoms in the channel leads to an increase in the average length and relative binding energy in silicene sheets. The bond length and energy in a defect-free silicene sheet have growth limits of approximately 2.48 Å and -4.52 eV, respectively. These values are achieved at a lithium to silicon ratio of ~ 1.

It is of interest to perform a cluster analysis of the lithium packings formed in and around the silicene channel. Let us use a purely geometric criterion for the formation of a cluster, assuming that the length of the Li-Li bond in a cluster cannot exceed 3.05 Å [29]. The criterion for the bonding of the Li atoms belonging to the cluster to the substrate was the condition that the length of the Li-Si bond should be less than 3.1 Å [30]. The cluster in contact with the

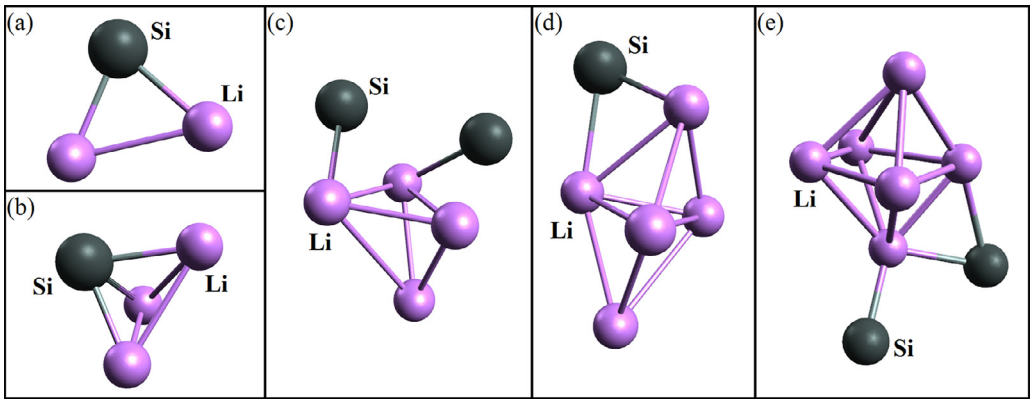

Fig. 7. Lithium clusters present in the model: (a) Li_2, (b) Li_3, (c) Li_4, (d) Li_5, and (e) Li_6; their bond with Si atoms (dark circles) belonging to the channel wall is shown.

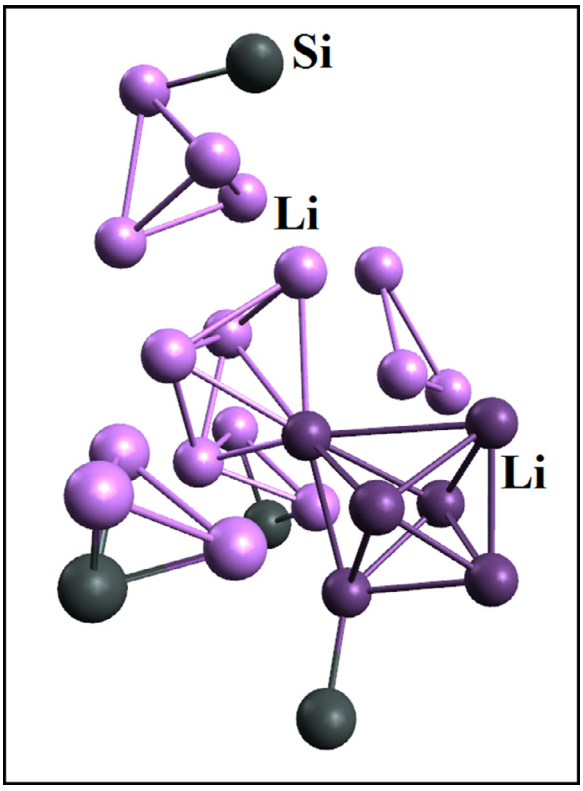

Fig. 8. The Li_n clusters selected in the model that fill the silicene channel upon adsorption of 84 lithium atoms by bilayer silicene; the connection of clusters with the channel walls is represented by Li-Si bonds of the cluster atoms with the nearest Si atoms in the wall.

channel wall must have at least one Li-Si bond. Obviously, the type of clusters being formed depends on the number of Li atoms filling or surrounding the channel at each specific moment of lithization. In Fig. 7 shows the clusters that can form in the system under study when more Li atoms are introduced into it, than: (a) 7, (b) 10, (c) 13, (d) 17, (e) 19. A further increase in the number of lithium atoms in the system up to 84 does not lead to the formation of clusters of a new type, but increases the number of isomers for the clusters shown in Fig. 7. Fig. 8 shows an example of filling the region in the channel with lithium during the adsorption of 84 Li atoms at bilayer silicene.

We carried out an additional study of the thermal stability of the Lin clusters (n = 2–6) selected in the model. Each of these clusters was extracted from the final configuration of the system, together with one of the silicene sheets, to which it was linked via Li-Si bonds. In other words, Li atoms not belonging to the cluster and the silicene sheet farthest from the cluster were removed from the system. Then, for the reduced system, geometric optimization was carried out using the generalized gradient approximation in the form of PBE, after that first principle molecular dynamic calculation was carried out in a Nose-Hoover thermostat in the temperature range from 300 to 500 K with a step of 50 K. The calculation duration at each temperature was 1000 time steps (Δt = 1 fs).

Geometric optimization led to the following results: 1) the Li_2 cluster disintegrated, and lithium atoms moved to positions above the centers of the hexagonal ring (hollow position); 2) clusters Li_5 and Li_6 were also transformed with the formation of isomers Li_4 and Li_5, respectively; moreover, one Li atom from the smaller cluster moved to a position above the center of the hexagonal ring.

As a result of a first principle MD calculation, the following was established: 1) the Li_3 isomer disintegrated at a temperature of 300 K, and the separated Li atoms took place above the centers of hexagonal silicon rings; 2) the Li_4 isomer proved to be stable up to a temperature of 450 K, but at a temperature of 500 K it disintegrated to get individual Li atoms, these atoms were adsorbed on silicene in the hollow positions; 3) the Li_5 isomer disintegrated in the temperature range 400–500 K into individual Li atoms, which were adsorbed on silicene.

Thus, after structural optimization and the 200 degree heating, none of the Li clusters isolated in the model of a lithium-filled silicene channel retained its integrity. The lithium clusters present in the model turn out to be metastable. In the process of delitization, they must decay into individual atoms, which will be removed one by one from the silicene channel.

Defective structures appearing upon the adsorption of 40, 44, 72, and 84 lithium atoms in the channel are shown in Fig. 9. The adsorption of 40 lithium atoms leads to rupture in the hexagonal silicon ring of the lower silicene sheet; the length of one of the three silicon bonds increases to 4.09 Å. An increase in the number of adsorbed lithium atoms to 44 leads to the rupture of two silicon rings (the Si-Si bond lengths reach 4.15 and 4.32 Å). A further increase in the number of lithium atoms in the system can lead to both the formation of defects (60, 72, and 84 lithium atoms in the system) and the restoration of the silicene structure (52, 68, and 76 lithium atoms in the system) after an attempt to create a defect. With a lithium to silicon ratio of 2.3 (84 lithium atoms), lithium breaks hexagonal silicon rings in both the lower and upper silicene sheets. In this case, the rupture in the upper wall of lithium occurs due to the rotation of the silicene supercell 3 × 3. The formation of relatively stable structures when the channel 52, 68, and 76 was filled with lithium atoms was associated with the placement of Li atoms added outside the channel, which slightly influenced the stability of silicene.

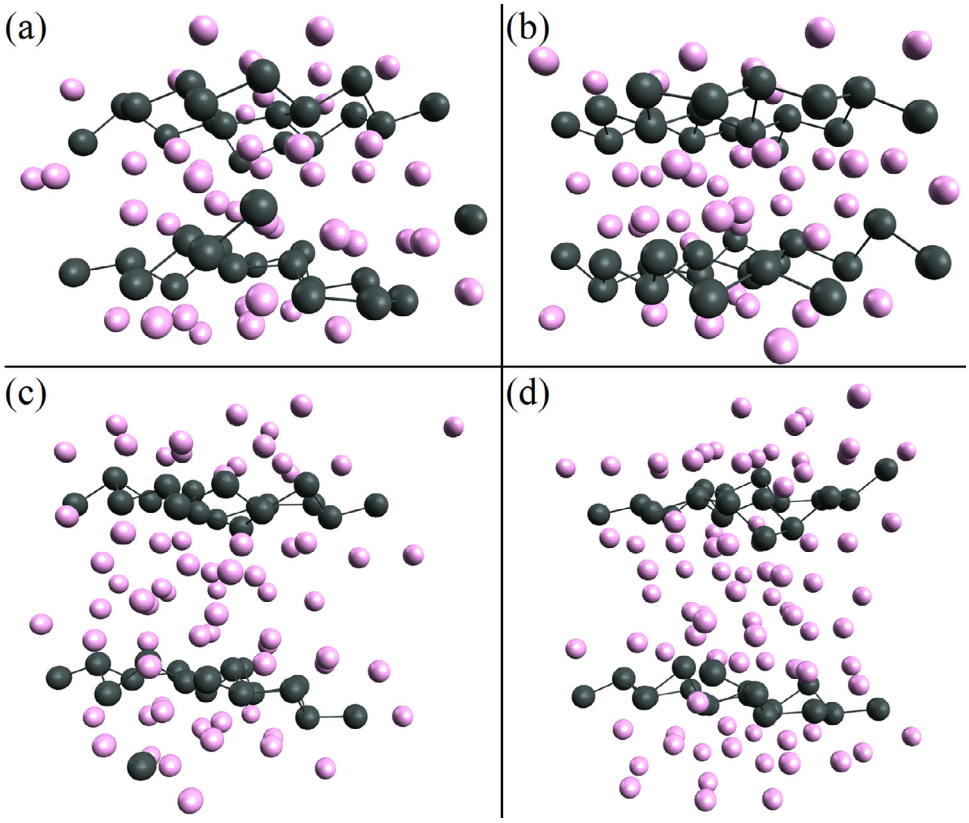

Fig. 9. The final geometric structure of the "silicene channel with lithium" system with the number of Li atoms: (a) 40, (b) 44, (c) 72, and (d) 84.

Thus, a perfect silicene channel does not collapse at all if the ratio of the number of Li / Si atoms = 1 (36 Li atoms are absorbed) or less than 1. In addition, the channel can become defective, but relatively stable if the ratio Li / Si <2.11 (the limiting number of adsorbed Li atoms is 76).

An increase in the lithium content in the channel can lead not only to the formation of defective silicene, but also to the redistribution of lithium in the channel. This is how lithium atoms can escape from the channel. Thus, 1 atom in the case of adsorption of 60 and 72 lithium atoms and 2 atoms in the case of adsorption of 68 left the channel. The emission of Li atoms does not occur when the channel is filled with 76 and 80 lithium atoms.

Fig. 10 shows the dependences of the cohesion energy, open-circuit voltage, the total Voronoi charge [31] transferred by lithium and the distance between the walls of the silicene channel on the ratio of lithium to the silicon atoms. It is seen that the cohesion energy is minimal at the ratio Li / Si = 1. When Li / Si > 1, there is a gradual increase in the cohesion energy associated with the enhancement of the interaction between lithium atoms. When calculating the specific gravimetric capacity of the system, three Li / Si ratios can be distinguished, which can be used in Eq. (5) in the form of the number of interacting electrons. The first value is 1. In this case, filling the silicene channel with lithium does not lead to the formation of defects in silicene. The second relation is 2.3. At this value of the Li / Si ratio, the maximum filling of the channel with lithium is reached. The third value 3.4 was obtained by approximating to zero the polynomial of the 4th degree, which describes the dependence of the specific cohesion energy between the lithium surfaces and the walls of the silicene channel on the Li / Si ratio. Substitution of these values into formula 3 gives the following gravimetric capacities of the systems: 1) 954.3, 2) 2223.5, and 3) 3244.6 mAh / g.

The total Voronoi elementary charge Q_V for lithium atoms has a maximum upon absorption of 44 lithium atoms. The drop in the total charge is associated with the onset of destruction of the silicene structure. In this case, lithium appears in the system, which does not interact with silicene. In other words, Li atoms appear, experiencing only Li – Li interactions. Fig. 11 shows the number of lithium atoms that do not interact with silicon atoms, but have only lithium bonds, depending on the Li / Si ratio. It is seen that the filling of the silicene channel with lithium leads to the appearance of lithium atoms that do not interact with silicon atoms. The number of Li atoms that do not interact with silicon atoms was estimated by analyzing the Li-Si "bond" lengths.

An increase in the number of lithium atoms in the system from 4 to 84 leads to an increase in the open circuit voltage (OCV) from 0.076 to 0.785 V, respectively. The OCV value for all considered ratios Li / Si does not exceed 1 V, which indicates the absence of metallic dendrites in the system [32]. However, as the extrapolation of the obtained OCV (Li / Si) dependence shows, a further increase in the amount of lithium in the system to the ratio Li / Si = 3 will lead to an increase in the open voltage to a higher value than 1V. Thus, at high values of the Li / Si ratio, dendrites can form in the system.

Recall that the initial width of the silicene channel was 7.5 Å. When the ratio of lithium to silicon changes from 0.1 (1) to 0.4 (4), the channel contracts, which enhances the interaction between silicon atoms of the upper and lower silicene sheets. With an increase in the number of lithium atoms in the channel up to the Li / Si ratio from 0.5 to 1.8, the distance between the channel walls changes from 3.079 to 7.088 Å. In this range of values of the channel gap, the interaction between the channel walls is minimized. When the Li / Si ratio is from 2 to 2.3 (3), the channel expands from 8.054 to 8.955 Å, i.e. it becomes wider than it was at the very beginning of the calculations. Knowing the change in the

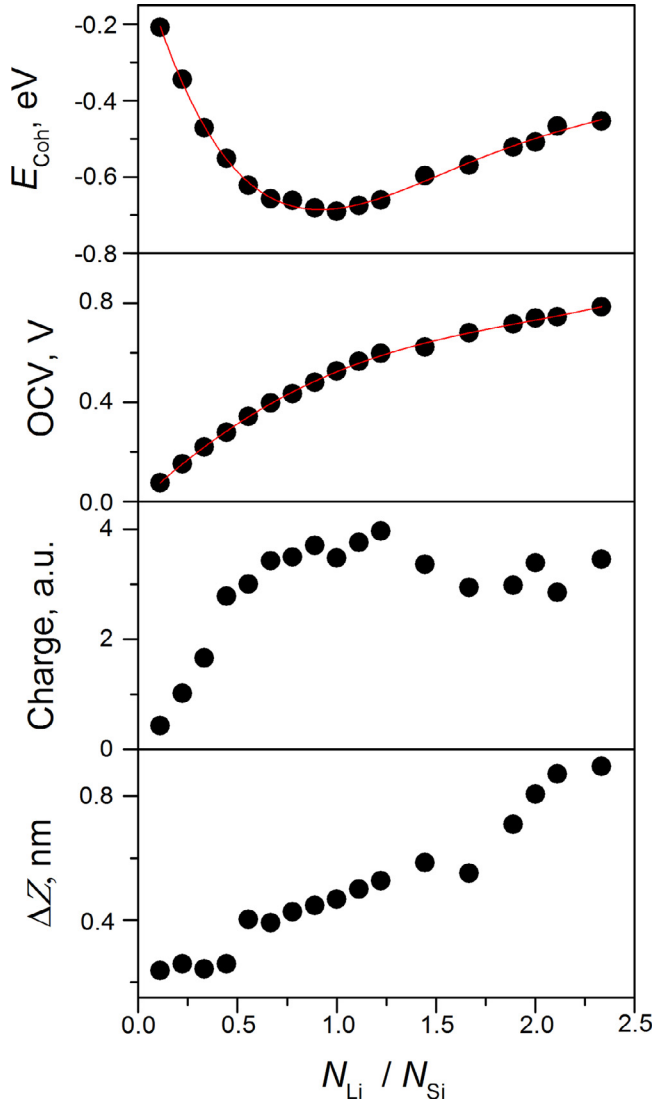

Fig. 10. Dependences of the cohesion energy between sheets of silicene and lithium surfaces, open voltage, total Voronoi charge transferred by lithium and the gap between the walls of the silicene channel on the ratio of lithium atoms to silicon atoms in the system.

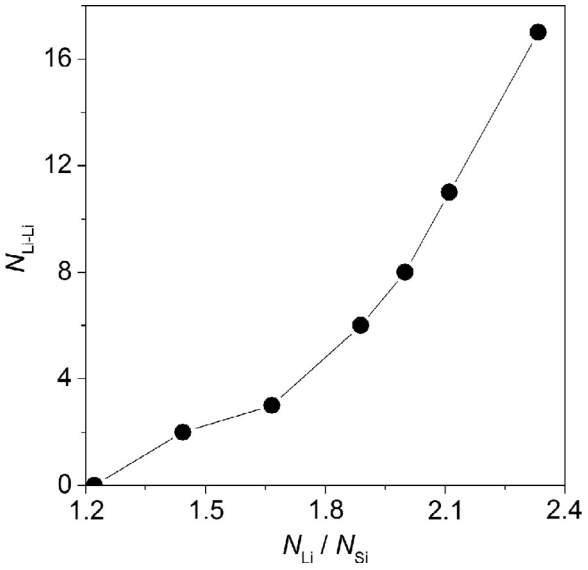

Fig. 11. Dependence of the amount of lithium that does not interact with silicon on the ratio of lithium atoms with silicon atoms in the system.

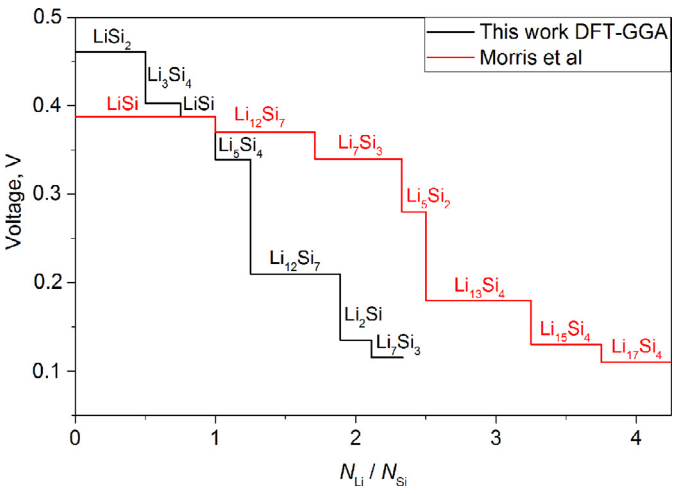

Fig. 12. Voltage profile plotted as a function of the ratio of lithium atoms to silicon atoms in the channel.

distance between the walls of the channel, we can calculate the change in the volume of the channel as:

$$V_N/V_4 = S\Delta Z(N)/S\Delta Z(4) = \Delta Z(N)/\Delta Z(4), \quad (8)$$

where V_N and V_4 are the volume of the silicene channel containing N and 4 lithium atoms, respectively, S is the area of the 3 × 3 silicene superlattice, and $\Delta Z(N)$ and $\Delta Z(4)$ is the distance between the silicene sheets upon adsorption of N and 4 lithium atoms, respectively.

The maximum physical absorption of lithium in a similar channel in the ratio of 1 Li to 15.7 Si was studied in the classical molecular dynamics model [33]. In this case, at Li / Si = 0.063, the change in the channel volume was 26%. In this work, the Li / Si ratio varied from 0.1 (1) to 1 and, while maintaining the defect-free channel, such a change in this ratio led to an increase in the channel volume by 97%. In the case of maximum channel filling, when Li / Si = 2.3, the increase in the channel volume was 278%.

During charging ion Li^+ moves from cathode to anode. Since the operating voltage of the battery is completely determined by the number of separated charges, the movement of a charged particle between the electrodes causes a change in the potential difference between them. The voltage profile obtained with this model when filling the silicene channel with lithium is shown in Fig. 12. As can be seen from the figure, the voltage decreases when lithium is added to the system according to the received sequence: $LiSi_2$, Li_3Si_4, LiSi, Li_5Si_4, $Li_{12}Si_7$ and Li_2Si. Fig. 9 also shows the voltage profile obtained using the DFT method in conjunction with the random structure searching method [34]. It can be seen that first principle MD calculations give a steeper descent of the voltage profile, so that V reaches values of ~ 0.1 V much faster. Flat areas with their corresponding phases were highlighted in the graph representing the results of this work, using the arithmetic mean of averaging close voltage values. Most of the Li-Si phases shown in the graph reflecting the results of this work were established in [20], where, as a result of first principle calculations, a stronger chemical interaction of lithium with silicene was shown in comparison with the interaction of Li-graphene. Using DFT calculations, the Li_5Si_4 compound was identified, which can be used as photovoltaic materials [35]. The Li_2Si phase is an amorphous shell formed during the initial intercalation of lithium into silicon [36].

The filling of the silicene channel with lithium affects the electronic properties of the system. Fig. 13 shows the band structures

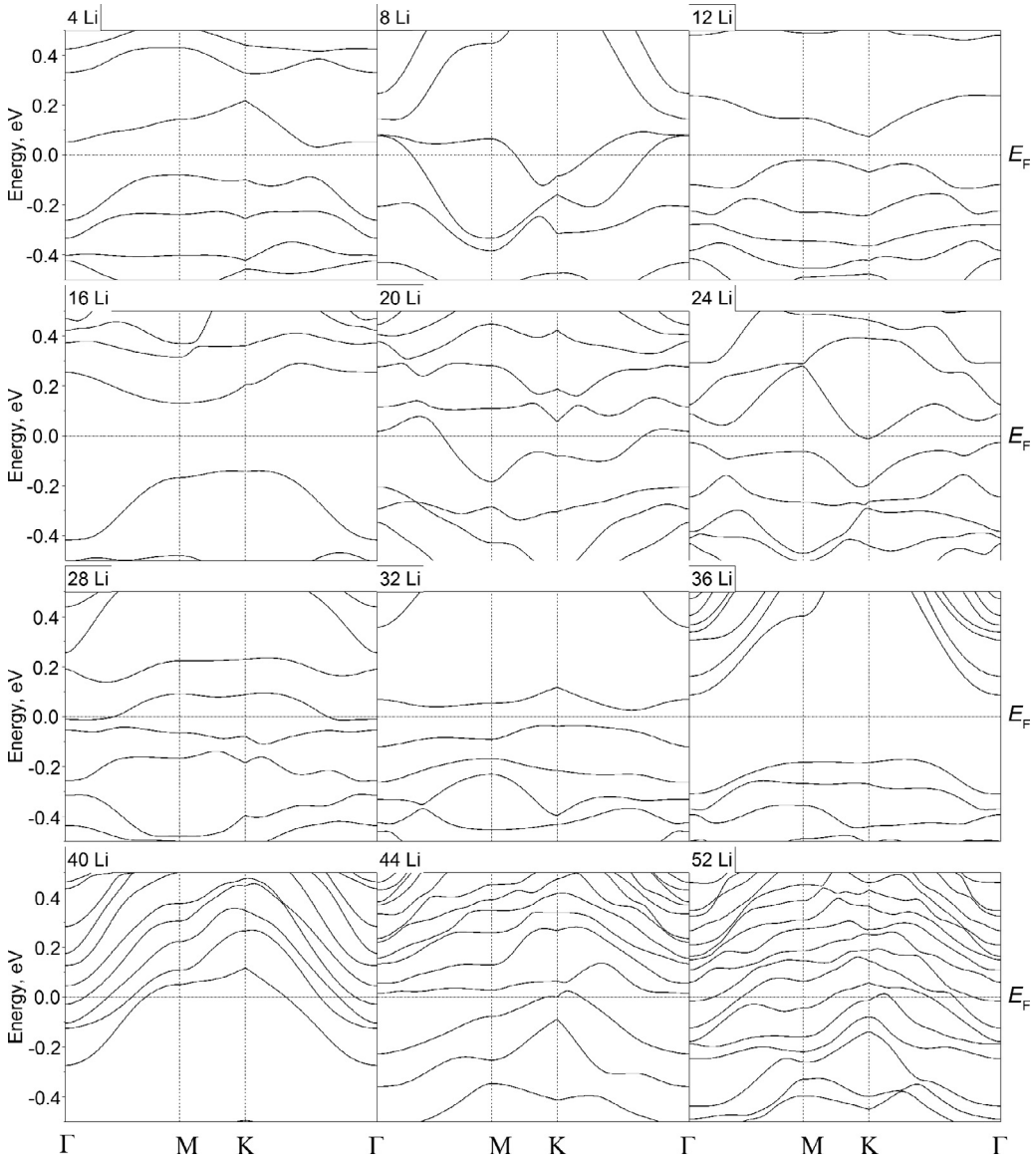

Fig. 13. Band structures of a silicene channel upon absorption of 4 to 52 lithium atoms onto it.

obtained for the silicene channel during the adsorption of 4 to 52 lithium atoms. It is seen that an increase in the lithium concentration in the channel leads to semiconductor-conductor and conductor-semiconductor transitions. When Li / Si = 1, the system acquires semiconductor properties with an indirect band gap of 0.244 eV. Earlier in [37, 38], it was reported that the adsorption of lithium on single-layer silicene in a 1:1 ratio leads to the appearance of semiconductor with a straight band gap of 0.388 eV. At a Li / Si ratio of 1.4 (52 lithium atoms), the system is finally metallized.

4. Discussion

The gravimetric capacity (954 mA • h / g) obtained in this work, which ensures the stability of an anode made of perfect two-layer silicene, turned out to be lower than the corresponding characteristic (1384 mA • h / g) calculated within the framework of classical molecular dynamics [15]. Perhaps this is due to the inaccuracy of the empirical potentials used and a different size of silicene sheets (each sheet of silicene contained 54 atoms) in [15]. In addition, we found that the silicene anode has unconfirmed stability up to a gravimetric capacity of 2223 mA • h / g. The anode was formed from a free-standing two-layer silicene. Real silicene can exist only on the substrate on which it is obtained. It was shown in [39] that the substrate stabilizes silicene. Therefore, it is quite possible that the actual achievable gravimetric capacity of the silicene anode will be higher than 954 mA • h / g.

DFT calculations predict the existence of various stable Li-Si phases [40–42]. Among them, Li_1Si_1, $Li_{12}Si_7$, Li_7Si_3, $Li_{13}Si_4$, $Li_{15}Si_4$, and $Li_{22}Si_5$. The presence of these phases was also confirmed using a DFT calculation with random structure searching in [34], in which one more phase $Li_{17}Si_4$ was also found. The methods used in [34, 40–42] determine the configurations of atoms corresponding to a temperature of 0 K; such an important factor as the effect of temperature on the stability of configurations was not taken into account here. First principle molecular dynamics calculations were not performed. Each of the found phases corresponds to local energy minima. Therefore, they can be considered as metastable compounds of lithium with silicon. In general, the question of how correctly the multiple phases, even metastable ones, are determined for Li-Si is still open. The point is that these "phases" were defined in too small systems. In this case, the locations of

individual atoms had a noticeable effect on the energy of the system, and the absence of molecular dynamics calculations did not allow obtaining equilibrium (relaxed) systems in each case. More accurately, the difference between Li-Si phases was determined using in situ X-ray diffraction [43]. In this experiment, it was shown that at the end of the lithiation process, the amorphous Li_xSi phase crystallized into the metastable $Li_{15}Si_4$ phase.

The energy stored by a battery E is given by:

$$E = \int V dQ_V = Q_V V \quad (9)$$

At the same level of the anode charging (up to $N_{Li} / N_{Si} \leq 2.3$), the energy stored by the battery, calculated from the voltage profile established in this work, turns out to be 7% less than one determined from the voltage profile of work [34].

In [41], the experiment was carried out at low (room) temperature. Cold nuclei of crystallization could form at the stage of formation of the amorphous phase. However, they could not cause the rapid crystallization described in the work. Since there is an activation barrier for the initiation of crystallization, external heating of the system is necessary for its passage, which was not there. Nevertheless, crystallization of an amorphous body is still possible at low temperatures, if a hot crystallization center appears in the system. The accidental appearance of a hot region is possible, for example, due to the local accumulation of nucleation centers of the crystalline phase [44]. The appearance of such a region stimulates more intense nucleation and accelerated growth of the crystalline phase with self-heating. It is this character of crystallization that is described in [43].

In [45], on the basis of model concepts, multistage phase transformations of crystallization - amorphization during the formation of various lithium-silicon phases as a result of cycling were considered. Based on model concepts, it is argued that the energy barriers separating the crystalline and amorphous phases are the main reason for the prolonged voltage plateau for silicon electrodes. According to the data obtained in the model, the initiation of crystallization is described using typical homogeneous nucleation. The presence of fragments of the crystalline phase of $Li_{15}Si_4$ in the corresponding amorphous phase is also allowed, which, as a rule, can be observed experimentally in various systems. However, the model does not explain the appearance of multiple specific Li-Si phases during lithization of a silicon electrode and does not consider the possibility of the local release of excess electrical energy required for the initiation of crystallization of the amorphous $Li_{15}Si_4$ compound.

Intensive research to improve the functionality of the thin film silicon anode continues. The procedure for the formation of amorphous thin lithium-silicon layers has shown itself as a promising approach to reducing significant losses in the capacity of the anode material [46]. The preliminary lithiation of thin silicon films to incorporate lithium into the electrode material makes it possible to increase the electronic conductivity of the electrode, reduce irreversible power losses in the first cycle, and stabilize the Coulomb efficiency. However, during cycling, the electrode surface is oxidized, forming a Li_xSiO_y film, which leads to a slow change in the electrochemical properties of the electrode.

Liquid electrolytes used in lithium ion batteries may contain compounds containing halogens, carbon, nitrogen, oxygen, and hydrogen, among them: LiN $(SO_2CF_3)_2$, $LiClO_4$, $LiPF_6$, $LiBF_4$, or $LiBH_4$. The liquid electrolyte is in direct contact with both the cathode and the anode. When charging the LIB, the anode is filled with lithium. If the anode material contains cavities, they are filled with Li atoms, which, due to the tendency to form a covalent bond, can form Li_n clusters [47]. A cationic cell in the form of a cluster easily attracts the anion (F^-, Cl^-) present in the electrolyte and establishes a strong electrostatic bond with it [47]. There is also a possibility of CLi_n, NLi_n, OLi_n, or H_mLi_n clusters forming. The stability of such clusters containing from 1 to 7 Li atoms was considered in [48–53].

5. Conclusion

In the present work, we studied the stability of the silicene anode with respect to its filling with lithium. The calculations are based on the DFT method and first principle molecular dynamics runs using a Nose -Hoover thermostat. The data obtained refer to a temperature of 293 K. The structural, energy, and electronic properties of a silicene channel filled with lithium from the inside and outside are calculated. The channel of perfect silicene remains stable when filled with lithium up to a gravimetric capacity of 954 mA h / g. However, the range of stability of the lithium-absorbed silicene channel can be expanded if the channel is located on a substrate. When the ratio of lithium to silicon is ~ 1, a minimum of cohesive energy is achieved between the surfaces formed by lithium and the silicene sheets, and the maximum bond stretching in the silicene sheets is also created. The absorption of lithium leads to a constant change in the electronic conductivity, so that there are semiconductor-conductor and conductor-semiconductor transitions.

The use of a silicene anode with a substrate can provide a 3–4 times higher charging capacity of lithium-ion batteries than is possible with a conventional graphite anode.

Declaration of Competing Interest

The authors declare that they have no known competing financial interests or personal relationships that could have appeared to influence the work reported in this paper.

Supplementary materials

Supplementary material associated with this article can be found, in the online version, at doi:10.1016/j.electacta.2021.138143.

Credit authorship contribution statement

A.Y. Galashev: Conceptualization, Writing – original draft, Writing – review & editing, Supervision. **A.S. Vorob'ev:** Writing – original draft, Formal analysis, Visualization.

References

[1] A. Molle, C. Grazianetti, L. Tao, D. Taneja, Md.H. Alam, D. Akinwande, Silicene, silicene derivatives, and their device applications, Chem. Soc. Rev. 47 (2018) 6370–6387.
[2] H. Lin, W. Qiu, J. Liu, Silicene: wet-chemical exfoliation synthesis and biodegradable tumor nanomedicine, Adv. Mater. 31 (2019) 1903013.
[3] J. Zhuang, X. Xu, G. Peleckis, W. Hao, S.X. Dou, Y. Du, Silicene: a promising anode for lithium-ion batteries, Adv. Mater. 29 (2017) 1606716.
[4] X. Zhang, X. Qiu, D. Kong, L. Zhou, Z. Li, X. Li, L. Zhi, Silicene flowers: a dual stabilized silicon building block for high-performance lithium battery anodes, ACS Nano 11 (2017) 7476–7484.
[5] X. Tan, C.R. Cabrera, Z. Chen, Metallic BSi 3 silicene: A promising high capacity anode material for lithium-ion batteries, J. Phys. Chem. C 118 (2014) 25836–25843.
[6] B. Jerliu, E. Hüger, L. Dörrer, B.-K. Seidlhofer, R. Steitz, V. Oberst, U. Geckle, M. Bruns, H. Schmidt, Volume expansion during lithiation of amorphous silicon thin film electrodes studied by in-operando neutron reflectometry, J. Phys. Chem. C 118 (2014) 9395–9399.
[7] S. Huang, T. Zhu, Atomistic mechanisms of lithium insertion in amorphous silicon, J. Power Sources 196 (2011) 3664–3668.
[8] M.J. Chon, V.A. Sethuraman, A. McCormick, V. Srinivasan, P.R. Guduru, Real–time measurement of stress and damage evolution during initial lithiation of crystalline silicon, Phys. Rev. Lett. 107 (2011) 045503.
[9] L.B. Chen, J.Y. Xie, H.C. Yu, T.H. Wang, An amorpheus Si thin film anode with high capacity and long cycling life for lithium ion batteries, J. Appl. Electrochem. 39 (2009) 1157–1162.
[10] V. Baranchugov, E. Markevich, E. Pollak, G. Salitra, D. Aurbach, Amorphous silicon thin films as high capacity anodes for Li-ion batteries in ionic liquid electrolytes, Electrochem.Commun 9 (2007) 796–800.

[11] F. Strauß, E. Hüger, P. Heitjans, V. Trouillet, M. Bruns, H. Schmidt, Li-Si thin films for battery applications produced by ion-beam co-sputtering, RSC Adv. 5 (2015) 7192–7195.
[12] T. Shirai, T. Shirasawa, T. Hirahara, N. Fukui, T. Takahashi, S. Hasegawa, Structure determination of multilayer silicene grown on Ag(111) films by electron diffraction: Evidence for Ag segregation at the surface, Phys. Rev. B 89 (2014).
[13] A.Y. Galashev, K.A. Ivanichkina, K.P. Katin, M.M. Maslov, Computational study of lithium intercalation in silicene channels on a carbon substrate after nuclear transmutation doping, Computation 7 (2019) 60–76.
[14] A.Y. Galashev, K.A. Ivanichkina, K.P. Katin, M.M. Maslov, Computer test of a modified silicene/graphite anode for lithium-ion batteries, ACS Omega 5 (2020) 13207–13218.
[15] A.Y. Galashev, K.A. Ivanichkina, Silicene anodes for lithium-ion batteries on metal substrates, J. Electrochem. Soc. 167 (2020) 050510.
[16] A.Y. Galashev, K.A. Ivanichkina, Computer study of atomic mechanisms of intercalation/deintercalation of Li ions in a silicene anode on an Ag (111) substrate, J. Electrochem. Soc. 165 (2018) A1788.
[17] A.Y. Galashev, K.A. Ivanichkina, Computational investigation of a promising Si–Cu anode material, Phys. Chem. Chem. Phys. 21 (2019) 12310–12320.
[18] A.Y. Galashev, K.A. Ivanichkina, Computer test of a new silicene anode for lithium-ion batteries, ChemElectroChem 6 (2019) 1525–1535.
[19] A.Y. Galashev, Yu.P. Zaikov, New Si–Cu and Si–Ni anode materials for lithium-ion batteries, J. Appl. Electrochem. 49 (2019) 1027–1034.
[20] S. Xu, X. Fan, J. Liu, D.J. Singh, Q. Jiang, W. Zheng, Adsorption of Li on single-layer silicene for anodes of Li-ion batteries, Phys. Chem. Chem. Phys. 20 (2018) 8887–8896.
[21] J.M. Soler, E. Artacho, J.D. Gale, A. Garcia, J. Junquera, P. Ordejon, D. Sanchez–Portal, The SIESTA method for ab initio order-N materials simulation, J. Phys.: Condens. Matter. 14 (2002) 2745.
[22] S. Cahangirov, M. Topsakal, E. Aktürk, H. Şahin, S. Ciraci, Two- and one-dimensional honeycomb structures of silicon and germanium, Phys. Rev. Lett. 102 (2009) 236804.
[23] J.P. Perdew, K. Burke, M. Ernzerhof, Generalized gradient approximation made simple, Phys. Rev. Lett. 77 (1996) 3865–3868.
[24] H.J. Monkhorst, J.D. Pack, Special points for Brillouin-zone integrations, Phys. Rev. B. 13 (1976) 5188.
[25] S. Nose, A unified formulation of the constant temperature molecular dynamics methods, J. Chem. Phys. 81 (1984) 511–519.
[26] M.S. Islam, C.A.J. Fisher, Lithium and sodium battery cathode materials: computational insights into voltage, diffusion and nanostructural properties, Chem. Soc. Rev. 43 (2014) 185.
[27] J. Zhuang, X. Xu, H. Feng, Z. Li, X. Wang, Y. Du, Honeycomb silicon: a review of silicene, Sci. Bull. 60 (2015) 1551–1562.
[28] J.E. Padilha, R.B. Pontes, Free-Standing Bilayer Silicene: The effect of stacking order on the structural, electronic, and transport properties, J. Phys. Chem. C 119 (2015) 3818–3825.
[29] G. Yang, X. Fan, Z. Liang, Q. Xu, W. Zheng, Density functional theory study of Li binding to graphene, RSC Adv. 6 (2016) 26540–26545.
[30] H. Kim, C.-Y. Chou, J.G. Ekerdt, G.S. Hwang, Structure and properties of Li-Si alloys: a first-principles study, J. Phys. Chem. C 115 (2011) 2514–2521.
[31] G.C. Fonseca, J.W. Handgraaf, E.J. Baerends, F.M. Bickelhaupt, Voronoi deformation density (VDD) charges: assessment of the Mulliken, Bader, Hirshfeld, Weinhold, and VDD methods for charge analysis, J. Comp. Chem. 25 (2003) 189–210.
[32] C. Eames, M.S. Islam, Ion intercalation into two-dimensional transition-metal carbides: global screening for new high-capacity battery materials, J. Am. Chem. Soc. 136 (2014) 16270–16276.
[33] A.E. Galashev, K.A. Ivanichkina, Computer modeling of lithium intercalation and deintercalation in a silicene channel, Rus. J. Phys. Chem. A 93 (2019) 765–769.
[34] A.J. Morris, C.P. Grey, C.J. Pickard, Thermodynamically stable lithium silicides and germanides from density-functional theory calculations, Phys. Rev. B 90 (2014) 054111.
[35] M. Rasukkannu, D. Velauthapillai, P. Vajeeston, Computational modeling of novel bulk materials for the intermediate-band solar cells, ACS Omega 2 (2017) 1454–1462.
[36] J. Rohrer, A. Moradabadi, K. Albe, P. Kaghazchi, On the origin of anisotropic lithiation of silicon, J. Power Sources 293 (2015) 221–227.
[37] H.O. Tim, A.A. Farajian, Stability of lithiated silicene from first principles, J. Phys. Chem. C 116 (2012) 22916–22920.
[38] A.Y. Galashev, A.S. Vorob'ev, Physical properties of silicene electrodes for Li-, Na-, Mg-, K-ion batteries, J. Solid State Electrochem. 22 (2018) 3383–3391.
[39] A.E. Galashev, O.R. Rakhmanova, K.A. Ivanichkina, Graphene and graphite supports for silicene stabilization: a computation study, J. Struct. Chem. 59 (2018) 877–883.
[40] V.L. Chevrier, J.R. Dahn, First principles studies of disordered lithiated silicon, J. Electrochem. Soc. 157 (2010) A392–A398.
[41] V.L. Chevrier, J.R. Dahn, First principles model of amorphous silicon lithiation, J. Electrochem. Soc. 156 (2009) A454–A458.
[42] V.L. Chevrier, J. Zwanziger, J.R. Dahn, First principles study of Li–Si crystalline phases: charge transfer, electronic structure, and lattice vibrations, J. Alloy Compd. 496 (2010) 25–36.
[43] J. Li, J.R. Dahn, An in situ x-ray diffraction study of the reaction of Li with crystalline Si, J. Electrochem. Soc. 154 (2007) A156.
[44] V.P. Skripov, V.P. Koverda, Spontaneous Crystallization of Supercooled Liquids (1984).
[45] Y. Jiang, G. Offer, J. Jiang, M. Marinescu, H. Wang, Voltage hysteresis model for silicon electrodes for lithium ion batteries, including multi-step phase transformations, crystallization and amorphization, J. Electrochem. Soc. 167 (2020) 130533.
[46] D. Uxa, E. Hüger, L. Dörrer, H. Schmidt, Lithium-silicon compounds as electrode material for lithium-ion batteries, J. Electrochem. Soc. 167 (2020) 130522.
[47] A. Unal, O. Ayin, A density functional investigation on Li_nI (n = 1–8) clusters, J. Cluster Sci. (2020), doi:10.1007/s10876-020-01810-x.
[48] S. Senturk, A density functional study of Li_nCl (n = 1–7) clusters, Z. Naturforsch. A 66 (2011) 372–376.
[49] A.K. Srivastava, N. Misra, Nonlinear optical behavior of Li_nF (n = 2–5) superalkali clusters, J. Mol. Model. 21 (2015) 305.
[50] M. Milovanovic´, S. Velic˘kovic´, F. Veljkovic´, S. Jerosimic, Structure and stability of small lithium-chloride Li_n-$Cl_m^{(0,1+)}$ (n ≥m, n = 1–6, m = 1–3) clusters, Phys. Chem. Chem. Phys. 19 (2017) 30481–30497.
[51] A. Unal, B. Kotan, A DFT based study of geometries, stabilities and electronic properties of Li_nF (n = 1–8) clusters, Main Group Chem. 17 (2018) 267–272.
[52] N.L. Moreira, B.G.A. Brito, J.N.T. Rabelo, L. Candido, Quantum Monte Carlo study of the energetics of small hydrogenated and fluoride lithium clusters, J. Comput. Chem. 37 (2016) 1534–1536.
[53] P.von.R. Schleyer, Are CLi_6, NLi_5, OLi_4, Etc, Hypervalent? In New horizons of quantum chemistry, in: Proceedings of the Fourth International Congress of Quantum Chemistry Held at Uppsala, Sweden, June 14–19, 1982, pp. 95–109.